Bulgarian Chemical Communications, Volume 51, Issue 1 (pp. 10-15) 2019

Effect of ultrasound waves intensity on the removal of Congo red dye from the textile industry wastewater by Fe_3O_4@TiO_2 core-shell nanospheres

H. Ghaforyan[1*], T. Ghaffary[2], S. Mohammadibilankohi[1], M. Hasanpour[1], M. Ebrahimzadeh[1], R. Pincak[3,4], M. Farkhan[1]

[1]*Department of Physics, Payame Noor University, P.O.BOX 19395-3697 Tehran, I.R. of Iran*
[2] *Department of Science, Shiraz Branch, Islamic Azad University, Shiraz, Iran*
[3] *Institute of Experimental Physics, Slovak Academy of Sciences, Watsonova 47,043 53 Kosice, Slovak Republic*
[4]*Bogoliubov Laboratory of Theoretical Physics, Joint Institute for Nuclear Research, 141980 Dubna, Moscow region, Russia*

Received, April 29, 2018; Revised, July 23, 2018

In this study, Fe_3O_4@TiO_2 core-shell nanospheres synthesized by a ultrasound-assisted co-precipitation method and their performance in removal of Congo red dye from industrial wastewater under ultrasonic waves were investigated. The structural and morphological properties of the nanospheres were studied by X-ray diffraction (XRD) and transmission electron microscopy (TEM). The XRD analysis confirmed the high purity of the nanospheres synthesized under ultrasound assistance. According to the TEM images, the diameters of Fe_3O_4@TiO_2 nanospheres were about 5 - 15 nm. The adsorption rate of the Congo red dye using these nanoparticles is significantly dependent on the sonicator power and the adsorption rate reached 100% at a power above 30 W.

Keywords: Ultrasound waves, Water treatment, Congo red, Nanoparticles, Core-shell nanospheres, Fe_3O_4@TiO_2.

INTRODUCTION

In recent years, shortage of water resources and the ever-increasing development of industrial units has increased the production of industrial wastewater and contaminated water resources, which is considered a major socioeconomic problem [1]. Chemicals affect water quality indices such as color, taste and smell. It is necessary to control such compounds because they may produce undesired carcinogenic substances such as trihalomethanes. Among various industries, textile, pulp and paper, pharmaceutical, and leather industries are major producers of dye pollutants due to the consumption of thousands of tons of dyes [2-4]. Most dyes are resistant to biodegradation processes. The presence of dyes in the wastewater from such industries prevents the sunlight from penetrating into the water and consequently reduces the rate of photosynthetic processes in surface water [5]. The removal of organic compounds from aqueous environments has been widely studied [6-10]. The most common methods for the removal of such compounds include ozonation [11], coagulation [12], ion exchange [13], biodegradation [14], use of membranes [15], and adsorption [16]. The high cost of advanced oxidation and membrane processes, the need for a large amount of coagulants and production of large volumes of sludge in the coagulation process to remove humic acids, and the low degradation efficiency are among the disadvantages of these methods. Therefore, the use of inexpensive and cost-effective methods for the removal of dyes from the wastewater of textile and dye manufacturing plants is of special importance in developing countries to maintain human and environmental health [17]. The use of adsorption process has received much attention as a simple and cost-effective method [18]. The adsorption process is known as the most suitable method for removing dye pollutants and improving the quality of industrial wastewater because of low cost, simple design, simple operation, and insensitivity to toxic materials [19]. Recently, magnetic particles have been extensively used as a new adsorbent due to magnetic properties and separability by magnets, large number of active surface adsorption sites, and high pollutant removal efficiency [20-22]. In this regard, iron oxide nanoparticles are known as an effective adsorbent for the removal of pollutants from aqueous environments and are widely used for the removal of organic pollutants and heavy metals from such environments [23]. Absalan *et al*. studied the removal of a reactive red dye from aqueous medium using surfactant-modified iron oxide nanoparticles. According to their results, more than 98% of the dye was removed using this method [24].

* To whom all correspondence should be sent:
E-mail: pasiran@gmail.com

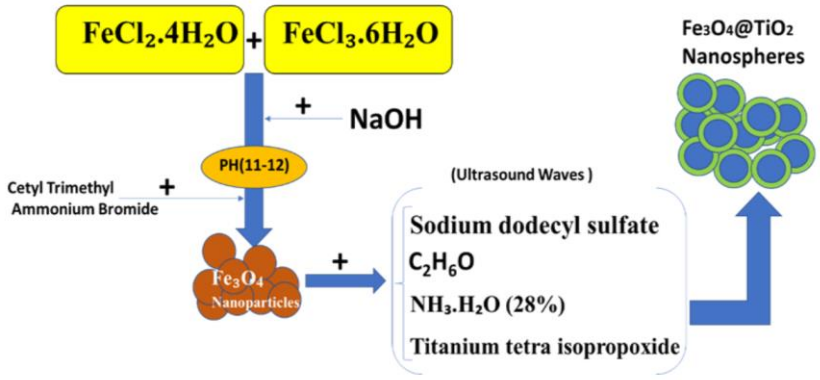

Figure 1. Schematics of the ultrasonic-assisted synthesis of Fe_3O_4@TiO_2 core-shell nanospheres.

Shen *et al*. conducted a study on the removal of nickel, copper, cadmium, and chromium ions and obtained a removal efficiency of more than 90% using iron oxide nanoparticles [25].The aim of the present study is to remove Congo red dye from the textile industry wastewater by synthesized Fe_3O_4@TiO_2 core-shell nanospheres in the presence and absence of ultrasound waves.

EXPERIMENTAL

Materials

All chemical reagents were purchased from Merck Chemical Co. $FeCl_3.6H_2O$, $FeCl_2.4H_2O$, cetyl trimethyl ammonium bromide (CTAB), sodium dodecyl sulfate (SDS), titanium tetra-isopropoxide (TTIP), 28% ammonium hydroxide solution, Congo red (CR), ethanol, hydrochloric acid and sodium hydroxide were used as received. Double distilled water (DDW) was used in all experiments.

Methods

First, 2.01 g of $FeCl_3.6H_2O$ and 0.7923 g of $FeCl_2.4H_2O$ were added to 40 ml of deoxygenated water purged with argon gas for 15 min. Once a transparent solution was obtained, 45.1 ml of 0.1 M sodium hydroxide solution was added to the mixture. Finally, the pH was adjusted in the range of 11-12. After precipitation, 0.1 g of CTAB was added to the solution as a surfactant. The resulting mixture was stirred using a magnetic stirrer at ambient temperature under continuous argon purge (Figure 1). After 20 min, the precipitate was separated using a magnet and washed firstly with water and dilute nitric acid and then with ethanol to remove impurities and reach neutral pH (7.0). The resulting precipitate was dried in an oven at 130°C for 30 min. Then, 0.7 g of CTAB or SDS was added to a mixture of 90 ml ethanol, 35 ml deionized water, and 3 ml 28% ammonium hydroxide. After that, 0.7 g of Fe_3O_4 prepared in the previous step was added to the resulting mixture. The mixture was further treated using a sonicator for 20 min. The sonication power was maintained at 20 W during mixing. A certain amount of TTIP was added to the mixture and further sonicated for an hour. The resulting precipitate was separated using a magnet and then washed several times with water and ethanol to remove impurities. The nanoparticles were then dried in an oven at 55°C for 5 h. Figure 1 shows schematically the ultrasonic-assisted synthesis of Fe_3O_4@TiO_2 core-shell nanospheres.

RESULTS

Figure 2 shows the XRD spectrum of the synthesized nanoparticles. The XRD analysis confirms the inverse spinel cubic structure of Fe_3O_4. The peaks appeared at 2θ = (220), (311), (400), (422), (511), and (440) are fully consistent with the standard cubic structure of the magnetic iron oxide (JCPDS, No. 19-0629). Obviously, Fe_3O_4 is the only phase detected in the XRD spectra and no characteristic peaks of ɣ-Fe_2O_3, another co-precipitation product with peaks very close to this structure, are observed. The Fe_3O_4 crystalline lattice consists of tetrahedral and octahedral sites in which iron ions are surrounded by 4 and 6 ions of oxygen, respectively. As can be seen, the peaks only correspond to the Fe_3O_4 structure, but the intensity of peaks is reduced due to overlapping of peaks. However, since no characteristic peaks of TiO_2 crystalline structure are observed, it can be concluded that amorphous titanium dioxide nanoparticles cover the Fe_3O_4 surface.

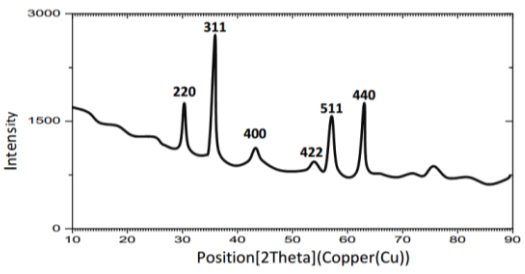

Figure 2. X-ray diffraction spectrum of iron oxide-titanium dioxide core-shell nanospheres.

Figure 3 shows the TEM image of Fe_3O_4@TiO_2 nanoparticles. Most particles are spherical with a mean diameter of 5-15 nm. It can be stated that the ultrasonic-assisted synthesis results in smaller Fe_3O_4@TiO_2 nanospheres showing a good agreement with XRD results.

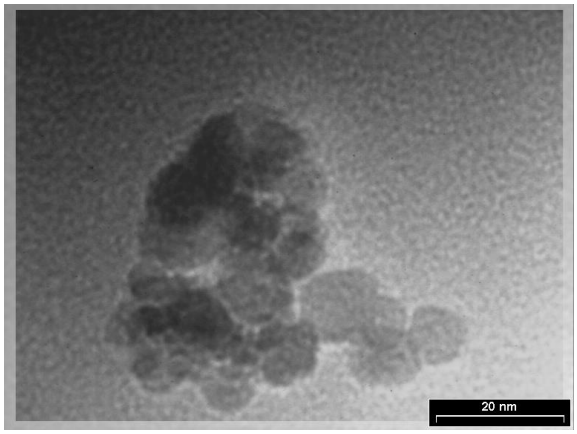

Figure 3. TEM micrograph of Fe_3O_4@TiO_2 nanoparticles synthesized under ultrasound assistance.

Removal of dye pollutants by Fe_3O_4@TiO_2 nanoparticles

To evaluate the performance of Fe_3O_4@TiO_2 nanospheres synthesized under ultrasound assistance in the removal of dye pollutants, a certain amount of the adsorbent was poured into the cell and mixed by a sonicator at a certain pH and temperature. Each experiment was repeated three times to verify the results. Figure 4 shows the chemical structure of Congo red dye. Dye removal was carried in different conditions. It is noteworthy that Congo red is one of the most widely used dyes in the textile industry. Because of its chemical structure, Congo red is among the stable and very toxic dyes in terms of degradability.

Effect of ultrasonic waves' intensity

The effect of various factors on the removal of Congo red dye from an aqueous solution of 150 mgr/l Congo red dye in deionized water (with an initial pH of 9-9.5) using the Fe_3O_4@TiO_2 adsorbent was studied. As clearly seen in Figure 5, dye removal decreases at low intensities but increases at intensities higher than 28 W. An increase in the number of bubbles at high ultrasonic intensities improves the cavitation process, which in turn significantly affects the mass transfer from the adsorbent surface. Therefore, the effect of other factors on the dye removal was studied at the optimal intensity of 28 W. The following chart was plotted using the sonicator power calculated by calorimetry.

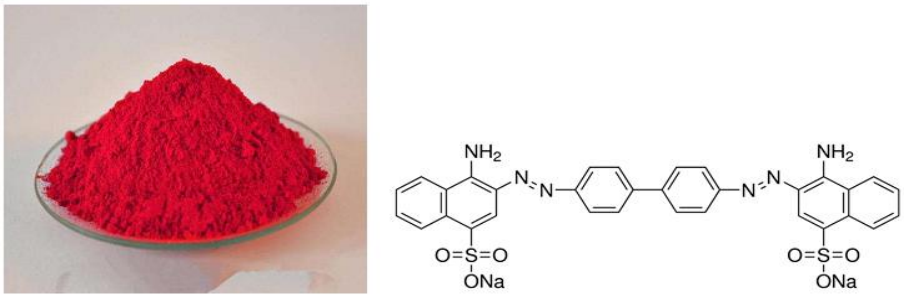

Figure 4. Chemical structure of Congo red dye

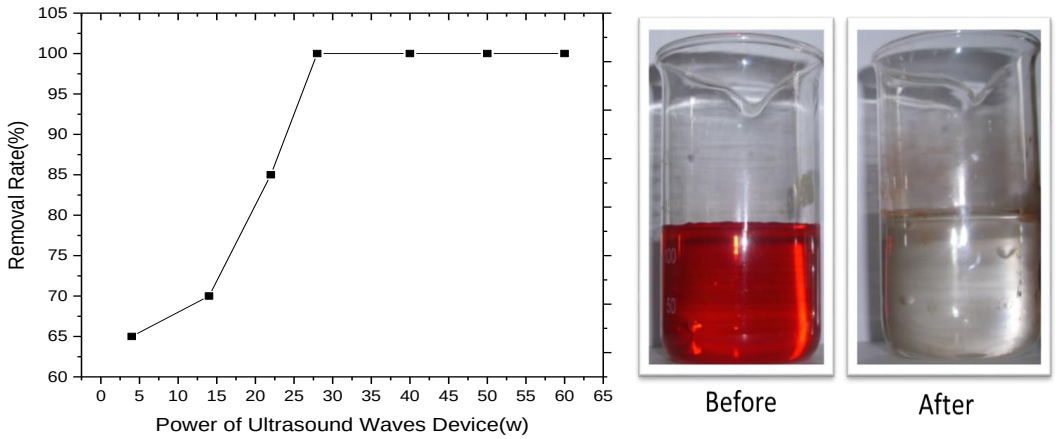

Figure 5. Effect of ultrasonic intensity on the removal of Congo red dye (concentration: 150 mg/l, adsorbent: 0.09 g, temperature: 21-24°C, time: 3 min).

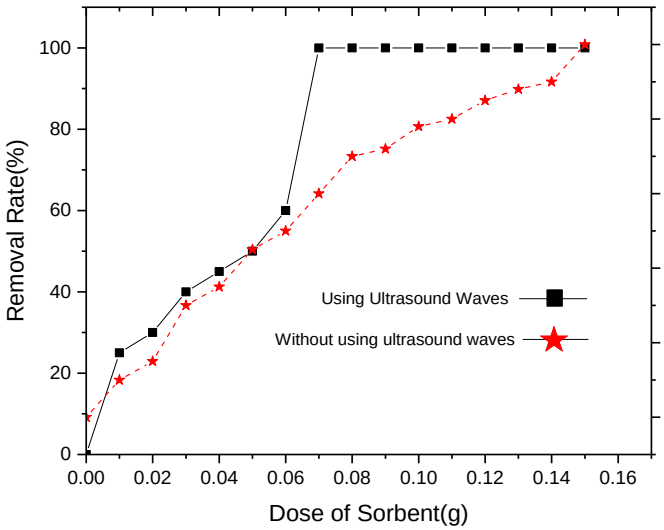

Figure 6. Effect of adsorbent concentration on Congo red dye removal (concentration: 150 mg/l, temperature: 21-24°C, time: 3 min)

The effect of different concentrations of the adsorbent (0.01 to 0.15 g) on the removal of Congo red dye from 65 ml of a 150 mg/l dye solution was studied at the initial pH of the dye for 3 min. As shown in Figure 6, with increasing the adsorbent level up to 0.15 g, the reaction rate in the classical method increases resulting in a dye removal percentage of 99.55%. The reaction rate also increases in the ultrasonic-assisted dye removal method with increasing the adsorbent level, but a dye removal rate of 99.7% was obtained with 0.09 g of Fe_3O_4@TiO_2 nanoparticles.

Since the amorphous structure of titanium dioxide contains Ti^{4+} and O^{2-} ions (based on the XRD results), the surface atoms cannot be fully coordinated leading to an increase in the degree of coordination unsaturation. Furthermore, surfactants may affect the arrangement of this configuration. The minimum configuration energy for the surface atoms occurs when they are in close contact with the surroundings at the atomic scale. With increasing degree of unsaturation, driving forces for chemical and physical adsorption will increase. The main driving forces for molecular adsorption include: (1) coordination of surface atoms with the surrounding atoms and (2) interaction of the surface charges with counter-ions. Obviously, an increase in the adsorbent level leads to an increase in the adsorption rate due to the increased contact surface of the adsorbent. With increasing adsorbent level, the contact surface of the adsorbent particles will increase. As a result, a larger number of dye molecules can be accomodated on the adsorbent surface leading to an increase in the adsorption rate. Moreover, the burst of cavitation bubbles causes the formation of high-pressure turbulent currents and high-speed microjets which reduce the size of larger particles. This in turn increases the contact surface and surface reactivity. In addition, the mass transfer process is improved by ultrasonically induced turbulence due to the mechanical pressures. Bubble bursting can also affect the surface diffusion and structure in this system. Therefore, an optimal adsorbent level of 0.1 g was used to investigate the effect of other factors.

DISCUSSION

According to the results, the initial intraparticle diffusion rate in the stirring method is higher than that of the ultrasonic method. This can be attributed to the larger thickness of the boundary layer in the ultrasonic method due to the increased number of dye molecules on the external surface of the adsorbent. Moreover, as temperature increases in the stirring method, intraparticle diffusion rate decreases due to increased ion mobility and eventually increased number of dye molecules in the boundary layer and on the external surface. In contrast, the intraparticle diffusion rate increases in the ultrasonic method because of accelerated mass transfer into the pores as a result of mechanical pressures.

CONCLUSION

It can be concluded that with increasing temperature, layer diffusion becomes the dominant mechanism in the presence or absence of ultrasonic waves. However, intraparticle diffusion is faster in the stirring method than in the ultrasonic method considering the boundary layer thickness. Nonetheless, the adsorption rate in these steps is very low compared to that on the surface. This can

be attributed to interactions between the dye molecules and the adsorbent surface. It is noteworthy that the dye-adsorbent interactions are stronger in the ultrasonic method.

Acknowledgements: *Thanks are due to the Payame Noor University in Iran for the financial support. Also, the work was partly supported by VEGA Grant No. 2/0009/16. R. Pincak would like to thank the TH division in CERN for hospitality.*

The authors declare no conflict of interests regarding the publication of this article.

REFERENCES

1. P. Rao, I. M. Lo, K. Yin, S. C. Tang, Removal of natural organic matter by cationic hydrogel with magnetic properties, *Journal of environmental management*, **92**(7), 1690 (2011).
2. T. A. Saleh, V. K. Gupta, Column with CNT/magnesium oxide composite for lead (II) removal from water, *Environmental Science and Pollution Research*, **19**(4), 1224 (2012).
3. J. Rivera-Utrilla, M. Sánchez-Polo, M. Á. Ferro-García, G. Prados-Joya, R. Ocampo-Pérez, Pharmaceuticals as emerging contaminants and their removal from water. A review, *Chemosphere*, **93**(7), 1268 (2013).
4. E. M. Dias, C. Petit, Towards the use of metal–organic frameworks for water reuse: a review of the recent advances in the field of organic pollutants removal and degradation and the next steps in the field, *Journal of Materials Chemistry* A, **3**(45), 22484 (2015).
5. S. M. Bilankohi, M. Ebrahimzadeh, T. Ghaffary, M. Zeidiyam, Scattering, Absorption and Extinction Properties of Al/TiO_2 Core/Shell Nanospheres, *Indian Journal of Science and Technology*, **8**(S9), 27 (2015).
6. I. Ali, Z. A. Alothman, A. Al-Warthan, Sorption, kinetic and thermodynamic studies of atrazine herbicide removal from water using iron nano-composite material, *International Journal of Environmental Science and Technology*, **13**(2), 733 (2016).
7. B. Wang, G. H. Huang, L. Liu, W. Li, Y. L. Xie, Integrated planning of urban water resources and water pollution control management: Case of Urumqi, China. *Journal of Water Resources Planning and Management*, **142**(6), 05016001 (2016).
8. N. Shah, F. Claessyns, S. Rimmer, M. Balal Arain, T. Rehan, A. Wazwaz, M. Wasi Ahmad, M. Ul-Islam, Effective Role of Magnetic Core-Shell Nanocomposites in Removing Organic and Inorganic Wastes from Water, *Recent Patents on Nanotechnology*, **10**(3), 202 (2016).
9. F. Meng, Q. Liang, H. Ren, X. Guo, Low-cost solvothermal synthesis of hierarchical structure γ-AlOOH and its application to remove Cr (VI), methyl orange and Congo red from contaminated water, *Current Nanoscience*, **11**(4), 434 (2015).
10. T. Huang, Adsorption of Trace Selenium on Nano-Ti2 from Natural Water Samples, *Current Analytical Chemistry*, **11**(3), 193 (2015).
11. D. Gümüş, F.Akbal, A comparative study of ozonation, iron coated zeolite catalyzed ozonation and granular activated carbon catalyzed ozonation of humic acid, *Chemosphere*, **174**, 218 (2017).
12. Y. Zhao, Y. Sun, C. Tian, B. Gao, Y. Wang, H. Shon, Y. Yang, Titanium tetrachloride for silver nanoparticle-humic acid composite contaminant removal in coagulation-ultrafiltration hybrid process: floc property and membrane fouling, *Environmental Science and Pollution Research*, **24**(2), 1757 (2017).
13. G. J. Millar, S. J. Couperthwaite, S. Papworth, Ion exchange of sodium chloride and sodium bicarbonate solutions using strong acid cation resins in relation to coal seam water treatment, *Journal of Water Process Engineering*, **11**, 60 (2016).
14. E. Baginska, A. Haib, K. Kümmerer, Biodegradation screening of chemicals in an artificial matrix simulating the water–sediment interface, *Chemosphere*, **119**, 1240 (2015).
15. J. M. Dickhout, J. Moreno, P. M. Biesheuvel, L. Boels, R. G. Lammertink, W. M. de Vos, Produced water treatment by membranes: A review from a colloidal perspective. *Journal of Colloid and Interface Science*, **487**, 523 (2017).
16. M. Chandrasekar, M. R. Ishak, S. M. Sapuan, Z. Leman, M. Jawaid, A review on the characterisation of natural fibers and their composites after alkali treatment and water absorption, *Plastics, Rubber and Composites*, **46**(3), 119 (2017).
17. L. Song, B. Zhu, V. Jegatheesan, G. Stephen, D. Mikel, S. Muthukumaran, A hybrid photocatalysis and ceramic membrane filtration process for humic acid degradation: Effect of pore size and transmembrane pressure, *Desalination and Water Treatment*, **69**, 102 (2017).
18. M. Y. Gaouar, B. Benguella, Efficient and eco-friendly adsorption using low-cost natural sorbents in waste water treatment, *Indian Journal of Chemical Technology (IJCT)*, **23**(3), 204 (2016).
19. L. Lin, X. Xu, C. Papelis, P. Xu, Innovative use of drinking water treatment solids for heavy metals removal from desalination concentrate: Synergistic effect of salts and natural organic matter, *Chemical Engineering Research and Design*, **120**, 231 (2017).
20. A. S. Adeleye, J. R. Conway, K. Garner, Y. Huang, Y. Su, A. A. Keller, Engineered nanomaterials for water treatment and remediation: costs, benefits, and applicability, *Chemical Engineering Journal*, **286**, 640 (2016).
21. M. Khan, I. M. Lo, Removal of ionizable aromatic pollutants from contaminated water using nano γ-Fe_2O_3 based magnetic cationic hydrogel: Sorptive performance, magnetic separation and reusability, *Journal of Hazardous Materials*, **322**, 195 (2017).

22. D. H. K. Reddy, Y. S. Yun, Spinel ferrite magnetic adsorbents: alternative future materials for water purification, *Coordination Chemistry Reviews*, **315**, 90 (2016).
23. L. Wang, C. Kim, Z. Zhang, Q. Hu, T. Sun, X. Hu, Adsorption Behavior of Lysozyme on Carbon-Coated Fe_3O_4 Nanoparticles, *Current Nanoscience*, **13**(2), 159 (2017).
24. A. Gharaati, M. Ebrahimzadeh, Enhanced Microwave Absorption Properties of FeCo@TiO_2 Core-Shell Nanoparticles, *Current Nanoscience*, **14**(6), 1 (2018).
25. A. M. Gutierrez, T. D. Dziubla, J. Z. Hilt, Recent advances on iron oxide magnetic nanoparticles as sorbents of organic pollutants in water and wastewater treatment, *Reviews on Environmental Health*, **32**(1-2), 111 (2017).